Current Trends in Technology and Science
ISSN: 2279-0535. Volume: 5, Issue: 6

# Influence of Incidence Angle on the Electrical Parameters of Vertical Silicon Solar Cell

**Gokhan SAHIN, Marcel Sitor DIOUF, Amary THIAM, Moussa Ibra NGOM, Ousmane DIASSE, Grégoire SISSOKO**
University of Cheikh Anta Diop, Dakar/Senegal, Faculty of Sciences and Techniques, Physics Department.
gsissoko@yahoo.com

**Abstract: -** In this paper, we present the study of a vertical junction silicon solar cell under frequency modulation monochromatic illumination, with incidence angle effect. Dealing with the continuity equation relative to excess minority carriers, the expression of carrier density versus both, frequency modulation and junction recombination velocity was established, for various incident angles this paper also has exhibited the Photocurrent density, photo voltage, and derived series and shunt resistances, and finally the space charge region capacitance.

**Keywords:** Vertical junction - Incidence Angle - Silicon solar cell - Frequency Modulation - Electrical parameters

## INTRODUCTION

The improvement of the solar cells is often limited by recombination of the excess minority carriers' photogene rated. Parameters and the control of technological process of manufacturing are significant during the conception of these devices. Several methods of characterization in static or quasi-static mode, as well as in transient state and/or dynamic frequency mode have been developed for the determination of one or several parameters **[1, 2, 3, 4, 5]**. In this regard we resolve continuity equation relative to excess minority carriers in the base. Solution takes account the wavelength, the frequency, the junction recombination velocity and the incidence angle. Then the I-V characteristic is derived and used to determine the electrical parameters such as series and shunt resistances, and the capacitance **[6]**.

## THEORY

Let us consider a silicon solar cell with parallel vertical junction N $^+$ P doped. This photovoltaic cell includes three parts: ***Emitter:*** frontal zone of N $^+$ type, it is doped with donor atoms. ***Base:*** zone of P type, it is doped with acceptor atoms. ***SCR:*** we find it between the emitter and the base and there reigns an intrinsic electrical field E which separates the electron-hole pairs. When the solar cell is illuminated under the incidence angle Θ, there is creation of electron-hole pairs in the base. Given that the contribution of the base to the photocurrent is larger than that of the emitter **[3, 4]**; the analysis will only concern the base region.

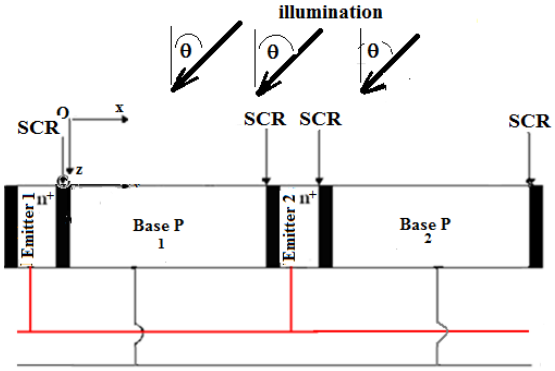


*Figure 1: Diagram of parallel vertical junction silicon solar cell*

In addition, we consider the hypothesis of Quasi-Neutral Base (Q.N.B) neglecting the crystal field within the solar cell. The distribution of the minority carrier's photogene rated (electrons) in the base is governed by the continuity equation. Taking into account the phenomena of generation-recombination and diffusion in the base, the continuity equation is given by the following equation **[7-10]**.

$$D(\omega)\cdot\frac{\partial^2\delta(x,\theta,t)}{\partial x^2}-\frac{\delta(x,\theta,t)}{\tau}=-G(z,\theta,t)+\frac{\partial\delta(x,\theta,t)}{\partial t} \quad (1)$$

D (ω) and τ are respectively, the diffusion constant and lifetime of excess minority carriers **[11]**. The excess minority carriers' density can be written as:

$$\delta(x,t)=\delta(x)\exp(-j\omega t) \quad (2)$$

Carrier generation rate G (z, θ, t) is given by:

$$G(z,\theta,\lambda,t)=g(z,\theta,\lambda)\exp(-j\omega t) \quad (3)$$

Were:

$$g(z,\theta,\lambda)=\alpha(\lambda)(1-R(\lambda))\cdot\phi(\lambda)\cdot \exp(-\alpha(\lambda)\cdot z)\cdot\cos(\theta) \quad (4)$$

x is the base depth along horizontal axis, ω is the angular frequency, θ is the incidence angle, z is the base depth according to the vertical axis; Sf is the junction

recombination velocity and λ the illumination wavelength.

If we replace equation (2) into equation (1), the temporary part is eliminated and we obtain the following expression:

$$\frac{\partial^2 \delta(x)}{\partial x^2} - \frac{\delta(x,\theta,t)}{L(\omega)^2} = -\frac{g(z,\theta)}{D(\omega)} \qquad (5)$$

The solution of this equation is:

$$\delta(x,\omega,\theta,z,Sf,\lambda) = A\cosh\left(\frac{x}{L(\omega)}\right) + B\sinh\left(\frac{x}{L(\omega)}\right) + \frac{L(\omega)^2}{D(\omega)} \cdot \alpha(\lambda)(1-R(\lambda)) \cdot \phi(\lambda) \cdot \exp(\alpha(\lambda) \cdot z) \cdot \cos(\theta) \qquad (6)$$

Coefficients A and B is determined through the following boundary conditions **[12]**:

- At the junction (x = 0):

$$D(\omega) \cdot \left.\frac{\partial \delta(x,\omega,\theta)}{\partial x}\right|_{x=0} = Sf \cdot \delta(x,\omega,\theta)|_{x=0} \qquad (7)$$

- At the middle of the base (x = H/2) **[13]**:

$$D(\omega) \cdot \left.\frac{\partial \delta(x,\omega,\theta)}{\partial x}\right|_{x=\frac{H}{2}} = 0 \qquad (8)$$

## RESULTS AND DISCUSSIONS

### a. *Minority Carriers Density:*

The figure 2 presents the profile of minority carriers' density versus horizontal depth x in base for various incidence angles:

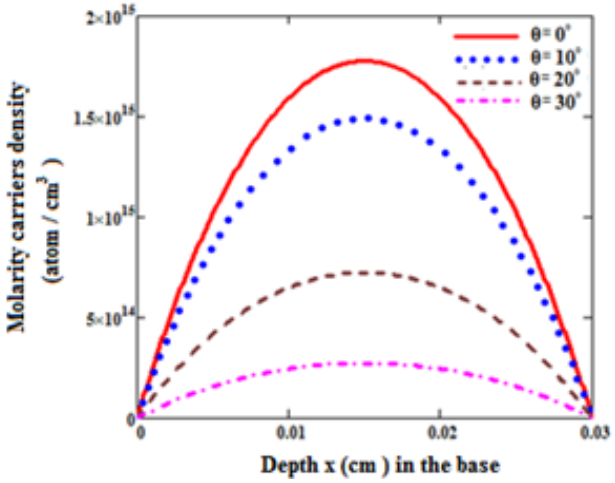


*Figure 2: Module of minority carrier's density versus depth x in the base for various incidence angles. Sf = 3.10³cm/s, H = 0.03 cm; $L_o$ = 0.02 cm, $D_o$ = 26 cm²/s, z = 0,0001 cm, λ = 0.52 µm, ω=10³rad/s.*

On this figure 2, we notice that the excess minority carriers' density in the base increases up to reach a maximum corresponding to a depth according to horizontal (x = H/2) in the base. At x superior to H/2, the density decreases up the limit of the depth (X = H) in the base. So, we note down three zones on the curve above following the depth x in the base:

i. Zone 1 (0 < x < H/2): where the gradient of the density of the carriers is positive. This translates the passage of electrons flow generating a photocurrent toward emitter-base junction;

ii. Zone 2: when x = H/2.

The module of the minority carrier's density in excess in the base is maximal and the gradient is nil, Minority carriers are stored.

iii. Zone 3 (H/2 < x < H): where the gradient of the minority carrier's density in the base is negative.

When the flow of incident light deviates from the perpendicular to the junction, we note that the minority carrier's density decreases for increasing incidence angle. Also, we note in Figure 2 that, at H/2, the minority carriers' density decreases when the incident angle of the illumination on the solar cell increases. This situation predicts the capacitive phenomena evolution.

### b. *Photocurrent:*

The photocurrent density is given by the following expression:

$$J_{Ph} = 2 \cdot q \cdot D(\omega) \cdot \left.\frac{\partial \delta(x,\omega,\theta)}{\partial x}\right|_{x=0} \qquad (9)$$

The profile of photocurrent density is given by figure3:

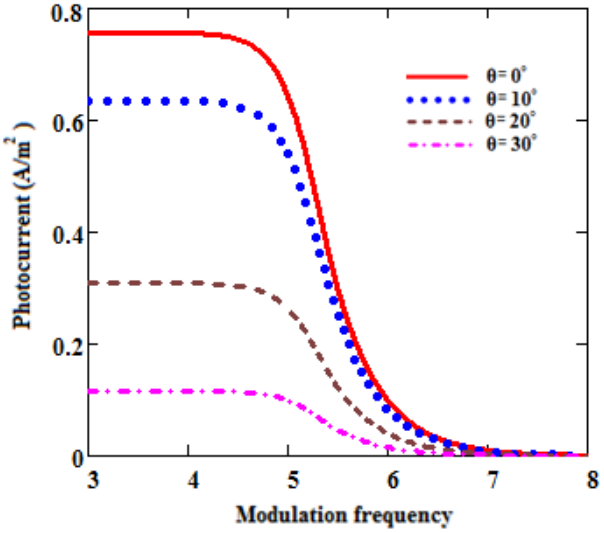


Figure 3: Module of the photocurrent density versus logarithm of the frequency for various incidence angles. Sf = 3.10³cm/s, H = 0.03cm, $L_o$=0.02 cm, $D_o$ = 26cm²/s, z = 0.0001cm, λ=0.52µm.

The photocurrent is maximal and is constant for the low values of the light frequency log (ω) < 5 (quasi-

static regime). For log (ω) > 5, the photocurrent decreases. This can be explained by the very high frequencies, the cell did not have time to relax. We also notice down that when the incident angle increases the amplitude module of the photocurrent density decreases. The variation of the photocurrent versus junction recombination velocity for various incidence angles is represented by the following figure:

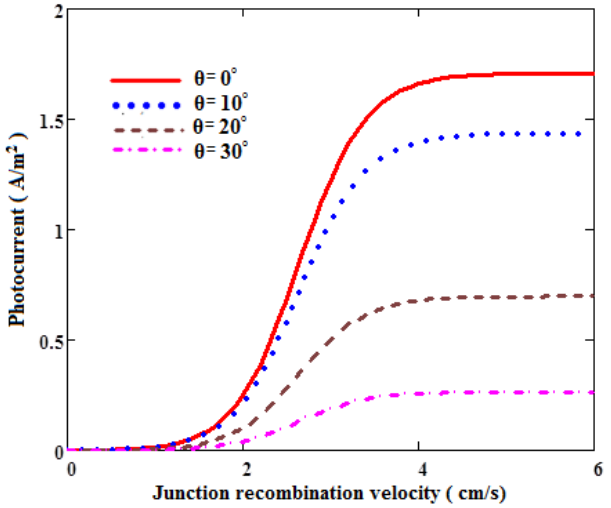


Figure 4: Module of the photocurrent density versus the junction recombination velocity for various values of the incidence angle. z = 0.0001cm, H = 0.03cm, $L_o$=0.02cm, $D_o$ = 26cm²/s, ω = 10³rad/s, λ = 0, 52µm

We can observe that we have two situations: one for low values of the junction recombination velocity and the other for the high values of the junction recombination velocity. For low values of junction recombination velocity, the photocurrent density is almost nil: this translates a situation of open-circuit. The junction recombination velocity characterizes the effects of interface in the base. It is explained by a loss of minority carriers. The module of the photocurrent density increases with the junction recombination velocity to reach the second bearing for high values of Sf corresponding to short circuiting. In this operating regime, the recombination linked to the interfaces remains but they are dominated by the strong diffusion of the minority carriers in the base toward the emitter hence their low influence upon the photocurrent.

c. ***Photo voltage:*** According to the BOLTZMANN relationship, the photo voltage is obtained by the expression (10).

$$V_{Ph} = V_T \cdot \ln\left[1 + \frac{Nb}{n_0^2} \cdot \delta(0)\right] \qquad (10)$$

with

$$V_T = \frac{K \cdot T}{q} \qquad (11)$$

Nb: doping rate in acceptor atoms in the base

$n_0$: is the intrinsic carrier's density related to the thermal stability.

K: the Boltzmann constant

T: the absolute temperature

q: elementary charge of the electron

The photo voltage profile for various values of the incidence angle is given by figure 5.

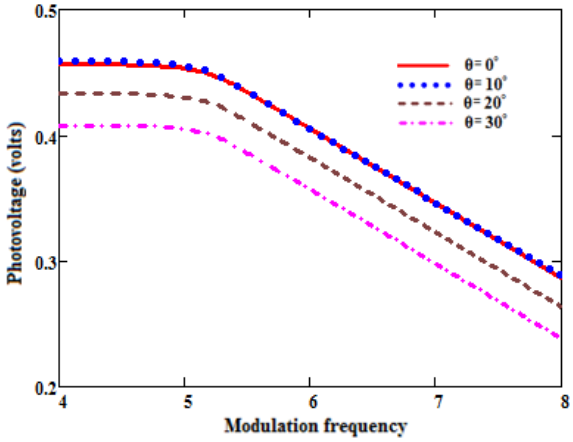


Figure 5: Module of the photo voltage versus the logarithm of the frequency for various incidence angles. ω=10³rad/s, Sf=3.10³cm/s, H=0.03cm, Lo=0.02cm, Do=26cm²/s, z = 0.0001cm, λ=0.52 µm

The photo voltage module remains maximal for the values of log (ω) < 5 and goes down for superior values. We can see that for the incident angle 0° < θ < 10° the module of the photo voltage sensibly keeps the same value and for θ > 10°, we can see a decrease in amplitude of the module of the photo voltage. The profile of Photo voltage versus the junction recombination velocity for incidence various angles is given upon figure 6: We note in figure 6 that photo voltage amplitude decreases when the incident angle increases. And for low values of the junction recombination velocity (Sf ≤ 3.10³ cm/s), the photo voltage is maximal and corresponds to the open-circuit situation. But for high values of junction recombination velocity (Sf ≥ 3.10³ cm/s), the photo voltage decreases gradually towards zero. It is explained that, for Sf ≤ 3.10³, carriers are stored at the level of the junction and for Sf ≥ 3.10³ cm/s, the junction is empty.

Current Trends in Technology and Science
ISSN: 2279-0535. Volume: 5, Issue: 6

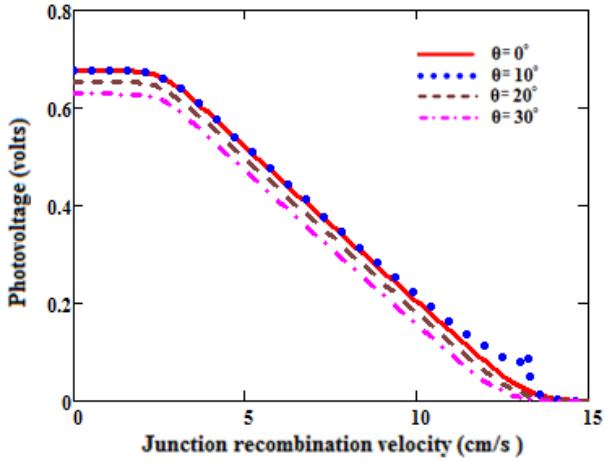


Figure 6: Module of the photo voltage versus the junction recombination velocity for various incidence angles. $\omega = 10^3$ rad/s, H = 0.03cm, $L_o$=0.02cm, $D_o$ = 26cm$^2$/s, z = 0.0001cm, $\lambda$ = 0.52µm

***d. I-V Characteristic:***

We present in figure 7 the photocurrent module profile versus the module of the photo voltage for incidence various angle.

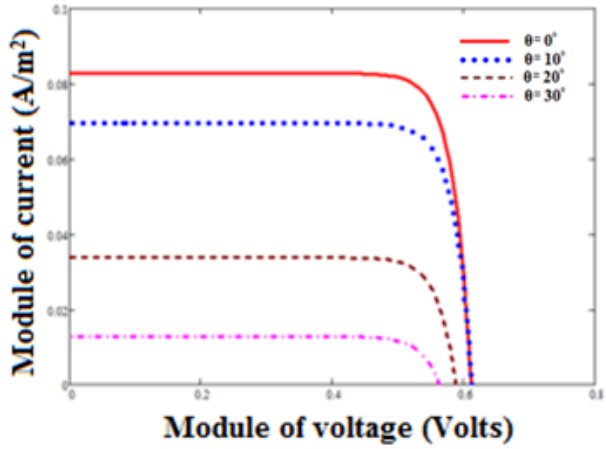


Figure 7: Characteristic current-voltage various incidence angles. $\omega = 10^3$ rad/s, H = 0.03cm, $L_o$=0.02cm, $D_o$ = 26cm$^2$/s, $\lambda$ = 0.52µm

For low tension values, the current is maximum and corresponds to the short-circuit situation; but when the tension turn toward that the open-circuit, the current gradually decreases. When the incidence angle increases, the amplitude decreases. From this characteristic, we can see that according to the operating regime of the solar cell in short-circuit or open-circuit situation, some electric parameters like resistances series and shunt can be determined from solar cell electrical model.

**e. *Series Resistance :***

The series resistance characterizes the resistive effects of material and the device of used contact. It represents the sum of the resistance in volume and at contacts. The figure 8 represents the I-V characteristic. We can see the voltage in open-circuit situation:

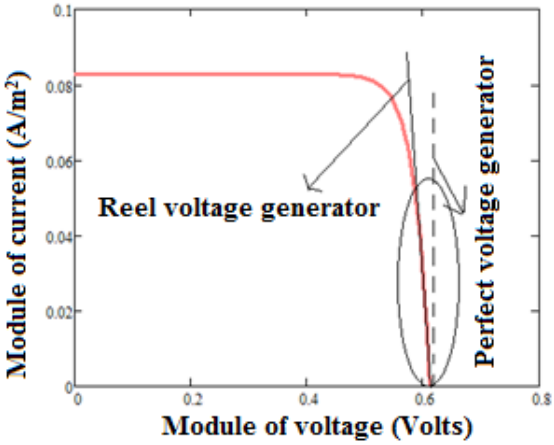


Figure 8: Characteristic current-voltage. $\omega = 10^3$ rad/s, H = 0.03cm, $L_o$ = 0.02cm, $D_o$ = 26cm$^2$/s, z = 0.0001cm, $\lambda$ = 0.52µm

The I-V characteristic set a bearing nearly vertical (figure 8) where the photo voltage lowly varies with the photocurrent. This relates a perfect voltage source. Really the solar cell presents some leaks. These are characterized by the presence in the equivalent circuit of a series resistance Rs **[19]**. The illustrative diagram of this device is given by figure 9:

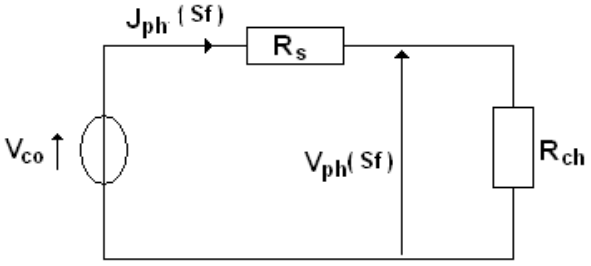


**Figure 9:** circuit électrique équivalent de la photopile en situation de circuit-ouvert.

Where:

- Jph (Sf) and Vph (Sf) are respectively the photocurrent and the photo voltage according to the junction recombination velocity;
- Rs and Rch respectively the series and charge resistances;
- Vco the open-circuit photo voltage.

We can deduce the series resistance Rs from the following expression **[14-18]** :

$$R_S(Sf) = \frac{V_{co} - V_{ph}(Sf)}{J_{ph}(Sf)} \qquad (12)$$

The profile of series resistance is given according to the junction recombination velocity for various incidence angles by figure 10:

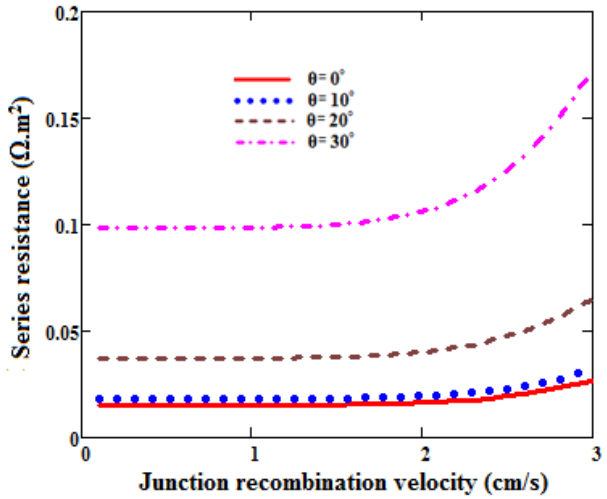


Figure 10: Module of series resistance versus the junction recombination velocity various incidence angles. ω = $10^3$ rad/s, H = 0.03cm, $L_o$ = 0.02cm, $D_o$=26cm²/s, z = 0.0001cm, λ = 0.52µm.

We note in figure 10 that series resistance increases with the junction recombination velocity and the amplitude of series resistance increases when incidence angle increases

***f. Shunt resistance:***

The shunt resistance comes from the recombination of the carriers in volume, on the surface and to the interfaces of a solar cell.

The figure 11 represents the I-V characteristic in a short-circuit situation:

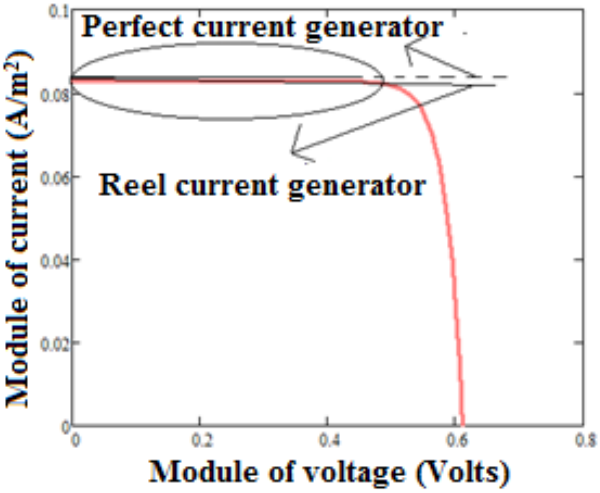


Figure 11: Characteristic current-voltage. ω = $10^3$ rad/s, H = 0.03cm, $L_o$ = 0.02cm, $D_o$= 6cm²/s, z = 0.0001cm, λ = 0.52µm.

I-V Characteristic presents a horizontal side which corresponds to situation where the photocurrent is independent of the photo voltage. These characteristics correspond to a perfect current source. This situation is comparable to the short-circuit photocurrent. As the solar cell is not ideal. These are characterized by the presence in the equivalent circuit of a shunt resistance Rsh **[20]**.

At figure 12, an electric circuit equivalent which correspondent to this mode is given:

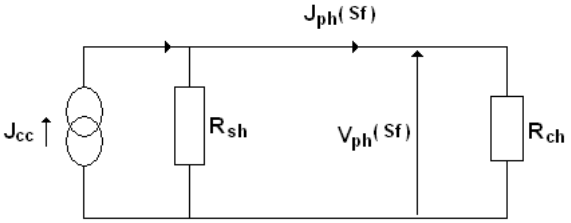


***Figure 12 : electric equivalent circuit in short-circuit situation***

Where:

- Jph (Sf) and Vph (Sf) are respectively the photocurrent and the photo voltage versus to the junction recombination velocity;
- Rsh and Rch respectively shunt resistance and load;
- Jcc the short-circuit photocurrent.

The expression of shunt resistance can be deduced by the following expression **[19]**:

$$R_{sh}(Sf) = \frac{V_{ph}(Sf)}{J_{cc} - J_{ph}(Sf)} \qquad (13)$$

Shunt resistance is represented according to the junction recombination velocity for different incidence angles on figure 13:

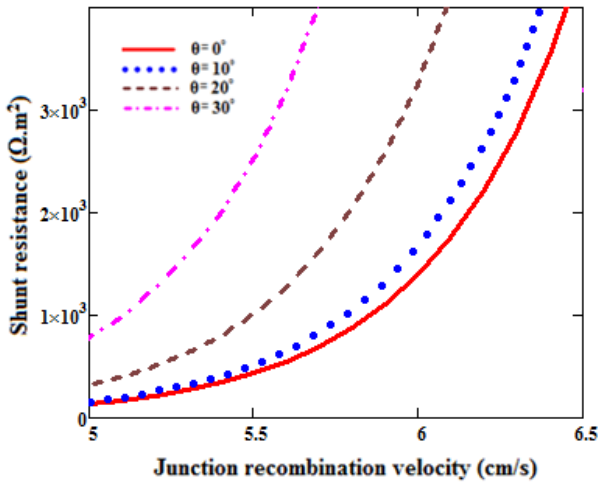


Figure 13: Module of resistance shunt according to the speed of recombination to the junction for various angles of incidence of the light. ω = $10^3$ rad/s, H =

0.03cm, $L_o$ = 0.02cm, $D_o$ = 26cm$^2$/s, z = 0.0001cm, λ=0.52µm

Figure 13 shows that shunt resistance increases with the junction recombination velocity. Shunt résistance amplitude increases either when the incident angle increased. We give some series and shunt resistance values for different incidence angles in Table 1:

Table 1 : Changes in series resistance and shunt values for different incidence angles at the junction recombination velocity.

| θ (°) | 0 | 10 | 20 | 30 |
|---|---|---|---|---|
| Rs (Ω.m²) | 0.015 | 0.018 | 0.037 | 0.098 |
| Rsh(Ω.m²) | 133 | 159 | 311 | 782 |

The table show that Rs and Rsh increases with increasing incident angle. This confirms the results obtained above. This may be due to shadowing phenomena. We took the value of the junction recombination velocity Sf = 7,149 cm.s$^{-1}$ for the series resistance, and for the shunt resistance Sf = 5.10$^5$ cm.s$^{-1}$.

***g. Capacitance***

When the solar cell is illuminated, there is generation and diffusion of minority carrier through the Space Charge Region (SCR), which is accompanied by charge storage.

The capacity equation is given by the relation 15.

$$C = \frac{dQ}{dVph} \qquad (14)$$

With

$$Q = q.\delta(x)\big|_{x=0} \qquad (15)$$

Figure 14 shows the variation of the capacity of Space Charge Region versus junction recombination velocity Sf for different incident angle values. When the incident angle increases, the capacitance amplitude decrease. And we show an Open circuit situation when the junction recombination velocity is low, the maximum capacity remains constant: there's a little mobility of the minority carriers who are found stored at vicinity of the junction. For Sf values greater than 2.10$^2$ cm.s$^{-1}$ we note a gradual decrease of the solar cell capacitance value which tends towards the short circuit situation. We are witnessing an expansion of the space charge zone between two limits corresponding to the open circuit conditions and short circuit of the solar cell.

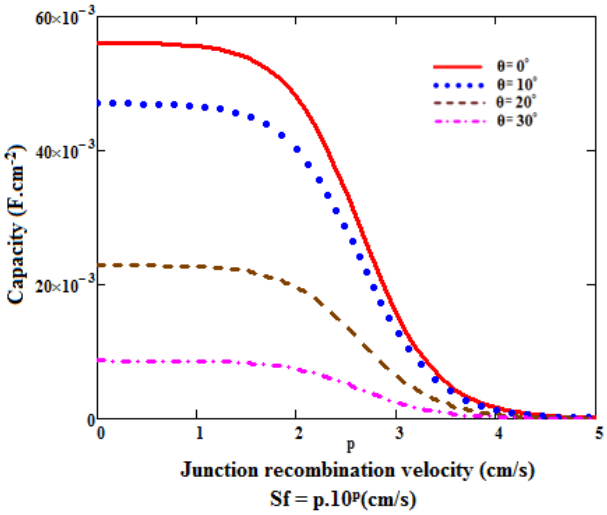


Figure 14: Module of SCR capacitance versus junction recombination velocity for various incident angles. ω = 10$^3$ rad/s, H = 0.03cm, $L_o$ = 0.02cm, $D_o$ = 26cm$^2$/s, z = 0.0001cm, λ = 0.52µm

## CONCLUSION

A theoretical study of a vertical junction solar cell has been presented. Electrical parameters such as photocurrent density, photo voltage, series resistances, shunt resistances, capacity and efficiency have been determined and we showed the behavior of solar cell versus modulation frequency and junction recombination velocity for various incidences angle. These parameters also decrease according to the modulation frequency by taking account the effect of the incidence angle. These parameters strongly depend on the modulation frequency and the incidence angle. This study exhibit the fact that photocurrent density, photo voltage and capacity do not depend on modulation frequency below a certain threshold which is the quasi steady state limit. Above that threshold photocurrent density, photo voltage and capacity decrease rapidly. It has also been shown that all the studied parameters depend on illumination incidence angle by a cosine law.

## REFERENCES

[1]. Saïdou Madougou, Mohamadou Kaka And Gregoire Sissoko Silicon Solar Cells: Recombination And Electrical Parameters Solar Energy, Book edited by: Radu D. Rugescu, ISBN 978-953-307-052-0, pp. 432, February 2010

[2]. M. M. DIONE, S. MBODJI, M. L. SAMB, M. DIENG, M. THIAME, S. NDOYE, F. I.BARRO, G. SISSOKO Vertical junction under constant multispectral light: determination of recombination Parameters Proceedings of the 24th European photovoltaic solar

energy conference and exhibition, Hamburg, Germany (sept 2009), 465 – 468.

[3]. M. L. SAMB, M. DIENG, S. MBODJI, B. MBOW, N. THIAM, F. I. BARRO, G. SISSOKO Recombination parameters measurement of silicon solar cell under constant white bias light Proceedings of the 24th European photovoltaic solar energy conference and exhibition, Hamburg, Germany, 2009, 469 – 472.

[4]. Lemrabott, Z.N. Bako, A. Wereme and G. Sissoko, 2012. Determination of the Recombination and Electrical Parameters of Vertical Multijunction Silicon Solar Cell. Res.J. Appl. Sci. Engineering Technol. Maxwell cientific Organization, 3(7): 602-611,

[5]. Orton, J.W. and P. Blood, 1990. The Electrical Characterization of Semiconductor: Meas urement of Minority Carrier Properties. Academic Press, London

[6]. Ahmed Yoro BA, Bakary Dit Dembo SYLLA, Ousmane SOW, Idrissa GAYE, Ndeye THIAM, Ibrahima LY, Recomination parameters measurement of silicon solar cell under constant white bias light with incident angle**,** Journal Current Trends in Technology and Science ISSN : 2279-0535, Volume: 3, Issue: 6 (Oct.- Nov. 2014)**,** pp 411-415**.**

[7]. Diallo. H. Ly, B. Dieng, I. Ly, M.M. Dione, M. Ndiaye, O.H. Lemrabott, Z.N. Bako, A. Wereme and G. Sissoko, 2012. Extermination of the Recombination and Electrical Parameters of Vertical Multijunction Silicon Solar Cell. Res.J. Appl. Sci. Engineering Technol. Maxwell cientific Organization, 3(7): 602-611, ISSN: 2040-7467.

[8]. Noriaki Honma and Chusuke Munakata ; sample thickness dependence of minority carrier Lifetimes Measured using an ac photovoltaic Method; Japanese journal of applied physics vol.26,no 12,December,1987,pp. 233-236

[9]. Noriaki HONMA ,Chusuke MUNAKATA and Hirofimi SHIMIZU; calibration of minority carrier lifetimes measured with an ac photovoltaic method; Japanese journal of applied physics vol.27,no 7,july,1988,pp. 1322-1326

[10]. Andreas Mandelis; Coupled ac photocurrent and photothermal reflectance response theory of semiconducting p-n junctions; J. Appl. Phys. 66(11), 1 December 1989,pp. 5572-5583

[11]. Dieng, A., I. Zerbo, M. Wade, A. S. Maiga and G. Sissoko, 2011. Three-dimensional study of a polycrystalline silicon solar cell: the influence of the applied magnetic field on the electrical parameters, Semi cond. Sci. Technol. 26 095023 (9pp)

[12]. Diallo, H. L., A. Wereme, A. S. Maiga and G. Sissoko, 2008. New approach of both junction and back surface recombination velocities in a 3D modeling study of a polycrystalline silicon solar cell, Eur. Phys. J. Appl. Phys. 42 203–11

[13]. Avraham GOVER, Paul STELLA**;** Vertical Multijunction Solar-Cell One-Dimensional Analysis; IEEE transactions on electron devices, vol. ed-21, no 6, June 1974, pp351-356.

[14]. Bashahu, M. and A. Habyarimana, 1995. Review and test of methods for determination of the solar cell series resistance, Renewable energy, 6, (2): 127-138.

[15]. Pysch, D., A. Mette and S. W. Glunz, 2007. A review and comparison of different methods to determine the series resistance of solar cells, Solar Energy Materials and Solar cells., 91 :1698-1706.

[16]. El- Adawi, M. K. and I. A. Al- Nuaim, 2002. A method to determine the solar cell series resistances from a single I-V characteristic curve considering its shunt resistance- new approach. Vacuum. 64: 33-36.

[17]. Mbodji, S., I. Ly, H. L. Diallo, M. M. Dione, O. Diasse and G. Sissoko, 2012. Modeling study of n+/p solar cell resistances from single I-V characteristic curve considering the junction recombination velocity (Sf). Res. J. Appl. Sci. Eng. Techno., 4(1): 1-7.